MEMS Simulation in Heavily Doped Silicon Devices

K. Matsuda* and Y. Kanda**

* Naruto University of Education, 748 Naruto, Tokushima, Japan,
matsudak@naruto-u.ac.jp
** Faculty of Engineering and Bio-nano Electronics Research Center, Kawagoe, Japan,
yozo@eng.toyo.ac.jp

ABSTRACT

Simulation of the semiconductor transport under heavily doped and stressed conditions is presented. The degenerate statistics are introduced by taking into account the density-of-state functions for the band tail and the impurity band. The momentum-dependent dielectric function is used for the dispersive screening and the carrier-carrier interaction which are appeared in the impurity scattering of the heavily doped silicon. The effects of mechanical stress on the conductivity are implemented by the relation between the stress and the Fermi energy, in which contributions of the carrier transfer and the mobility change for each of the splitted bands are included. As an application of this modeling, simulations for piezoresistive sensors are presented.

Keywords: MEMS, heavily doping, mobility, piezoresistance

1 INTRODUCTION

Effects of heavily doping and build-in stress become important in high density devices. The reason of the former is that the scaling rules allow the doping concentration to increase by the scaling factor, and that of the latter is the interface problems in layers or materials. In order to design and analyze these devices, the heavily doping effect and the stress-induced effect should be implemented in the MEMS simulation. It is expected for such simulation to determine the parameters for doping control in the manufacture of the micro pressure sensors so that the temperature noise of their piezoresistance (PR) gage can be reduced.

In the present paper, we propose a model for implementation of the heavily doped effects and the mechanical effects in the electrical transport equations.

2 THEORY

Most of the semiconductors have the many-valley conduction band and the degenerate valence band. Their conductivity is expressed by the summation of carrier concentration and mobility over all valleys or bands, depending on the carrier type; $\sigma = e\sum_i n^{(i)}\mu^{(i)}$. Not only the quantities in this equation but also all physical quantities of semiconductors can be calacterized by the impurity concentrations and the temperature $A(N_D, N_A, T)$, or indirectly by a Fermi energy $A(F)$. In other words, the semiconductor is considered as a system defined by these internal parameters. If we apply an external parameter such as the field or the stress etc. on this system, some of its physical quantities will be affected by it through the Fermi energy, which should be detected as a signal in the application to the sensors. Therefore it is necessary in the modeling of micro semiconductor sensors to figure out the relation between the external parameter and the Fermi energy.

Fractional change of the conductivity (σ) caused by the stress is called PR coefficeint and generally expressed as

$$\frac{1}{\sigma}\cdot\frac{\partial\sigma}{\partial P} = \frac{1}{n\mu}\sum_i\left(\frac{dn^{(i)}}{d\eta^{(i)}}\mu^{(i)} + n^{(i)}\frac{d\mu^{(i)}}{\partial\eta^{(i)}}\right)\frac{d\eta^{(i)}}{dP} \quad (1)$$

where P is the stress, $\eta^{(i)}$ is the relative reduced Fermi energy measured from i-band edge, $\mu = \sum_i \mu^{(i)}$, and $n^{(i)}$ and $\mu^{(i)}$ are the carrier concentration and mobility of i-band, respectively. For n-type material all valleys in conduction band are equivallent. Then Eq.1 becomes,

$$\frac{1}{\sigma}\cdot\frac{\partial\sigma}{\partial P} \approx \frac{1}{\sigma}\frac{d\sigma}{d\eta}\sum_i\frac{\mu^{(i)}}{\mu}\frac{d\eta^{(i)}}{dP} \quad \text{(for } n\text{-type)} \quad (2)$$

$$\approx \frac{1}{\sigma}\frac{d\sigma}{d\eta}\frac{\zeta-1}{\zeta+1}\frac{d\eta_h}{dP} \quad \text{(for } p\text{-type)} \quad (3)$$

where index h indicates the heavy hole, ζ is defined by the mobility ratio of light hole to heavy hole. The stress-induced shifts of the relative reduced Fermi energy are expressed as,

$$\frac{d\eta^{(i)}}{dP} = \frac{1}{3kT}\Xi_u\{(e_i-e_j)+(e_i-e_k)\} \quad \text{(for } n\text{-type)}$$

$$\frac{d\eta_h}{dP} = \frac{1}{kT}\sqrt{\epsilon_e} \quad \text{(for } p\text{-type)}$$

where

$$\epsilon_e = \frac{b^2}{2}[(e_1-e_2)^2+(e_2-e_3)^2+(e_3-e_1)^2]+\frac{d^2}{4}(e_4^2+e_5^2+e_6^2)$$

$i,j,k = 1,2,3$, e_j's are the components of strain tensor in the conventional contraction, Ξ_u is the uniaxial de-

formation potential of conduction band, b and d are the deformation potentials of valence band [1], [2].

The summation in Eq.2 and corresponding factor in Eq.3 at room temperature are defined as the PR coefficients for lower limit in the impurity concentration, which depend only on the crystallographic direction. Their factor $\frac{1}{\sigma}\frac{\partial\sigma}{\partial\eta}\frac{300}{T}$ is called PR factor and gives the dependency of impurity concentration and temperature [3]. If we use Fermi-Dirac approximation, the conductivity becomes proportional to $\mathcal{F}_{s+1/2}(\eta)$, where $\mathcal{F}_j$ is the Fermi integral of order j, s is the exponent appeared in the relaxation time $\tau = \tau_0 E^s$. Then the PR factor is expressed as,

$$\text{PR Factor} = \frac{300}{T}\frac{\mathcal{F}_{s-1}(\eta)}{\mathcal{F}_{s+1}(\eta)} \tag{4}$$

which is derived by adopting the relation of the Fermi integral; $\frac{d\mathcal{F}_j(\eta)}{d\eta} = \mathcal{F}_{j-1}(\eta)$. However, discrepancy between the calculation by this approximation and the experimental results of Yamada *et al.* are very large in heavily doped region [4]. Here we present a transport model in MEMS and its feasibility is demonstrated by solving this problem.

3 METHODS

3.1 Fermi Energy

Fermi energy is solved from the equation of charge neutrality condition by the Newton iteration scheme. For high impurity concentrations, density-of-state (DOS) function for the conduction (or valence) band and the impurity band DOS are taken into account. Once the Fermi energy is obtained, the carrier and ionized impurity concentrations can be determined from a given temperature. The screening length which is defined by the ionized impurity concentrations and appreared as the standard deviation in the band tail of DOS function and the impurity band DOS, is solved consistently. The numerical method is given in our previous paper [5].

3.2 Mobility model

Li *et al.* [6] have shown the numerical calculation of the carrier mobility in silicon by combining lattice, ionized impurity and neutral scattering. We have proposed a development for their method by using the results of subsection 3.1, in which the total relaxation time was obtained by adding the reciprocal relaxation time for each process according to the Mathiesson's rule, and by averaging it over the distribution of carrier energy. Here we make a further improvement for the Brooks-Herring (B-H) formula, which includes the momentum-dependent dielectric function (Lindhard dielectric function) and second Born approximation to simulate the dispersive screening and carrier-carrier interaction appeared in the impurity scattering of heavily doped silicon [7], [8]. The improved formula is expressed by,

$$\tau_I = \frac{(2m^*)^{3/2}(kT)^{1/2}N_I}{4\hbar^2}\left(\frac{e^2}{\epsilon}\right)^2 \int_0^\infty \frac{1}{[q^2+\beta^2 M(\xi,\eta)]^2} \times\left(1+\frac{\sin(qR)}{qR}\right)\sin\theta(1-\cos\theta)d\theta \tag{5}$$

where $M(\xi,\eta)$ is the screening function,

$$M(\xi,\eta) = \frac{1}{\mathcal{F}_{1/2}(\eta)}\frac{1}{\xi\sqrt{\pi}}\int_0^\infty \frac{x}{1+\exp(x^2-\eta)}\ln\left|\frac{x+\xi}{x-\xi}\right|dx \qquad (\xi^2 = \hbar^2q^2/8m^*kT)$$

N_I is the ionized impurity concentration, β^2 is the Thomas-Fermi screening length and R is the average distance between neighboring impurities: $R = (2\pi N_I)^{1/3}$. Overall scheme for the MEMS simulation in heavily doped silicon is shown in Figure 1 which includes the modefied carrier tranport calculation in the device simulation.

More easy way to implement the carrier mobility is the use of its formula with empirical paremeters. Major empirical modelings for carrier mobility are explained in the literature of Selberherr [9]. However, they cannot reproduce the experimental data in wide range extending to the heavily doped region. To improve this problem, Masetti *et al.* [10] gave formulae at 300 °K. Because we need the mobility formulae as a simultaneous function of impurity concentration and temperature, the formulae given by Arora *et al.* [11] are adopted to compare with our model.

3.3 Effects of mechanical stress

Effects of stress on the conductivity comprise two parts. The first part is the effects on the carrier concentrations. The mechanical stress splits the valleys of conduction band and the degenerate bands of valence band. As a result, part of the carriers in higher valleys (or bands) transfer to lower valleys (or bands). Thus the intrinsic distribution of electrons among these valleys is broken. Because the equi-energy surface of the valleys in conduction band has an ellipsoidal aspect and that of the splitted bands in valence band has either of two effective masses which depend on the stress and the direction of conductivity, this re-distribution of carriers causes an anisotropy in the conductivity.

The second part is the effects on the carrier mobility which include the carrier scattering and the conductivity effective mass. Because the strength of the carrier scattering is proportional to the final states density of the scattered carrier, only *f*-type intervalley (or interband) scatterring makes direct contribution to this effects. It can be proved from this fact that the stress-induced shift of the relaxation time in a valley (or band) is proportional to the shift of the carrier concentration, that is,

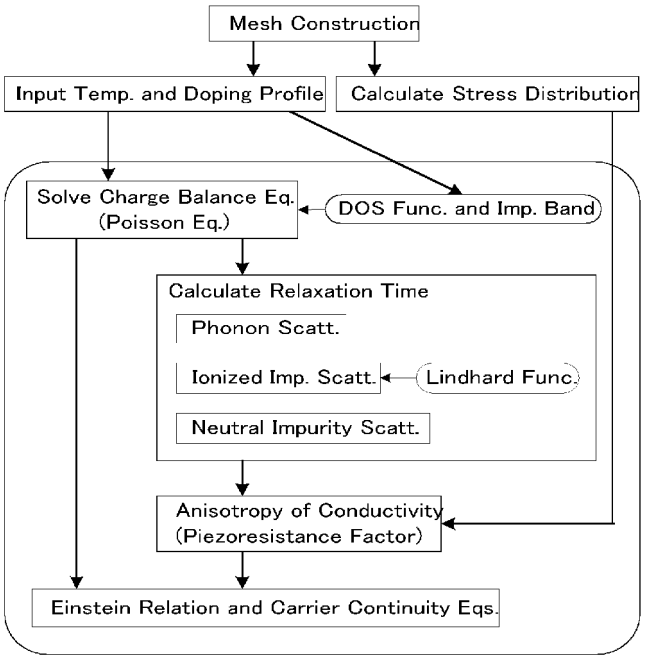

Figure 1: Flow-chart of the modefied carrier transport calculation in the device simulation.

the transfered part of the carriers in the valley (or band) [12].

Then we can define the stress-induced effects on the conductivity as a function of the internal parameters or a Fermi energy. The reduced Fermi energy derivatives of the physical quantities in Eqs.2 and 3 can be generally expressed as,

$$\frac{dA(N_D,N_A,T,P)}{d\eta} = \left(\frac{\partial A}{\partial N_D}\right)\left(\frac{d\eta}{dN_D}\right)^{-1} + \left(\frac{\partial A}{\partial N_A}\right)\left(\frac{d\eta}{dN_A}\right)^{-1} + \left(\frac{\partial A}{\partial T}\right)\left(\frac{d\eta}{dT}\right)^{-1} \quad (6)$$

4 RESULTS AND DISCUSSION

Result of the calculations for the electron mobilty at 300°K which use the Lindard dielectric function in the formula for the impurity scattering of the relaxation time is shown in Figure 2, comparing with the calculations by the B-H formula and the formula of Arora *et al.* As shown in this figure, the discrepancy of the result of Lindard model and those of other models becomes larger as the donor concentration increases. Similar figure for the hole mobility is shown in Figure 3. The behaviors of the mobility by using the Lindard model are similar for both type carriers. However the present calculation for the hole mobility at high acceptor concentrations is lower than the experimental data by Masetti *et al.* [10]. The reason for this discrepancy may be ascribed to the difference of the atomic form factor of the acceptors used in our calculation for the Lindard function.

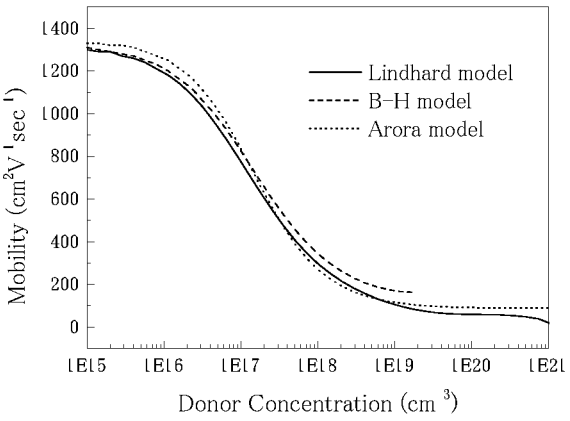

Figure 2: Electron mobility at 300 °K.

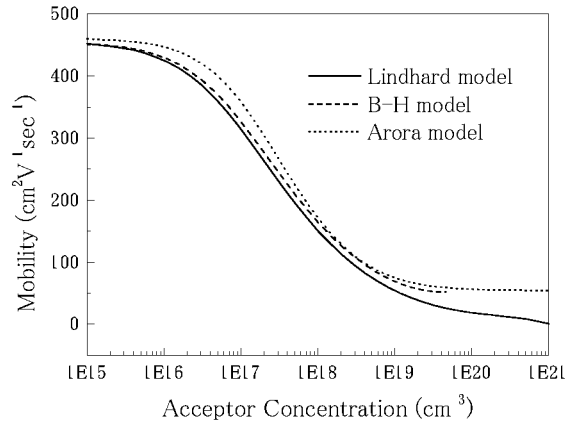

Figure 3: Hole mobility at 300 °K.

We shall use these mobility models to confirm their feasibility of the implementation in a temperature-dependent MEMS simulation. For this purpose, the temperature coefficient of the PR effect (TCPR) is considered as an application of our model. The TCPR is calculated from the PR factor by applying the calculation result of the mobility to eq.6 numerically.

The calculation results of TCPR for n-type and p-type silicons are shown in Figures 4 and 5, respectively. The most familiar expression for the conductivity of semicondoctors is the Fermi-Dirac approximation. The PR factor is initially introduced in Ref.[3] by using the Fermi-Dirac approximation. The curves indicated as "Fermi-Dirac approx." in these figures are reproduced from Eq.4. The present work revises our previous simulation model mainly in two points. One is that the Lindard function is used for the impurity scattering. The other is that the total differentiation as described in Eq.6

is considered in the differentials of carrier concentration and mobility. The curves indicated as "Lindard model" in these figures are the calculations by taking into account these two points. The curves indicated as "B-H model" and "Previous work" in these figures are the calculations by use of the B-H formula, but the latter is not considered the total differentiation. The caclulation by applying the mobility formula of Arora *et al.* to Eq.6 is denoted as "Arora model".

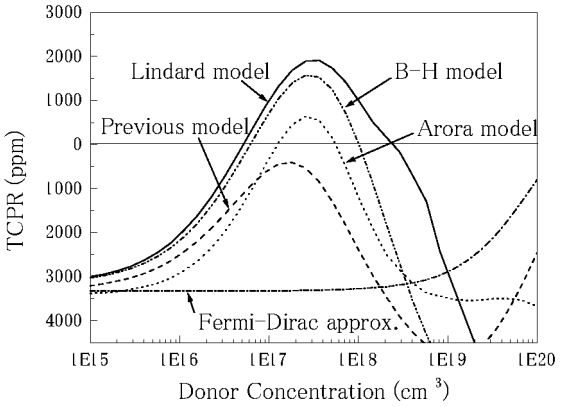

Figure 4: Temperature coefficient of the piezoresistance coefficient for n-type silicon at 300 °K. For the Fermi-Dirac approximation, phonon scattering ($s = -1/2$) is adopted.

As shown in Figure 4, the TCPR of n-type silicon has a peak at about 3×10^{17} cm^{-3} and becomes positive in the donor concentration range between 5×10^{16} and 3×10^{18} cm^{-3}. As the impurity concentration decreases the TCPR of both type materials becomes about 3300 ppm which is inversely proportional to the room temperature. The heavily doped effect on the carrier scattering, which is included in the Lindard model, makes the peak broaden to the higher impurity concentrations side.

Similar tendencies are found for p-type silicon. As shown in Figure 5, the peak of TCPR for p-type silicon is located at about 1×10^{18} cm^{-3} which is higher than that of n-type in the impurity concentration. The present models can reporduce the experimental data of Yamada *et al.* fairly well. The peak of TCPR calculated by taking into account the total differentiation shifts to the higher concentration side.

The reason why the behavior of TCPR in the Fermi-Dirac approximation is rather different from that of other models at higher impurity concentrations should be attributed to the fact that this approximation assumes the scattering just in isotropic parabolic energy bands.

In coclusion, we would like to comment that our approach for the mobility is valid for low field and does

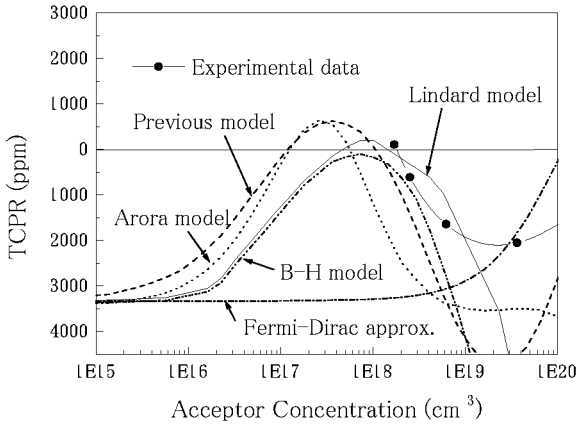

Figure 5: Temperature coefficient of the piezoresistance coefficient for p-type silicon at 300 °K. For the Fermi-Dirac approximation, phonon scattering ($s = -1/2$) is adopted. The experimental data of Yamada *et al.* are shown as a comparison [4].

not consume so much computational resources as Monte Carlo simulation. However, more accurate formula for the mobility is needed for the practical algorism in the transport simulation of MEMS.

REFERENCES

[1] M. Sweid, K. Hess and K. Seeger, J. Phys. Chem. Solids, 39, 393-402, 1978.

[2] K. Suzuki, H. Hasegawa and Y. Kanda, Jpn. J. Appl. Phys., 23(11), L871-L874, 1984.

[3] Y. Kanda, IEEE Trans. Electron Devices, ED-29(1), 64-70, 1982.

[4] K. Yamada, M. Nishihara, S. Shimada, M. Tanabe, M. Shimazoe and Y. Matsuoka, IEEE Trans. Electron Devices, ED-29(1), 71-77, 1982.

[5] K. Matsuda and Y. Kanda, Proc. the Third Int'l Conf. on MSM, San Diego, CA, USA, March 27-29, 2000, 605-608.

[6] S. S. Li and W. R. Thurber, Solid-State Electron., 20, 609-616, 1977.

[7] D. K. Ferry, "Semiconductors", Macmillan, 1991.

[8] H. Koshina and G. Kaiblinger-Grujin, Solid-State Electron., 42(3), 331-338, 1998.

[9] S. Selberherr, "Analysis and Simulation of Semiconductor Devices," Springer-Verlag, 1984.

[10] G. Masetti, M. Serveri and D. J. Roulston, IEEE Trans. Electron Devices, ED-30(7), 764-769, 1983.

[11] N. D. Arora, J. R. Hauser and D. J. Roulston, IEEE Trans. Electron Devices, ED-29(2), 292-295, 1982.

[12] R. W. Keyes, Solid State Phys., 11, 149-221, 1960.